06

Numerical modeling of carbides behavior under high-energy loading

© K.K. Maevskii[1,2]

[1] Lavrentyev Institute of Hydrodynamics, Siberian Branch, Russian Academy of Sciences, Novosibirsk, Russia
[2] Novosibirsk State University, Novosibirsk, Russia
e-mail: konstantinm@hydro.nsc.ru

Received July 1, 2021
Revised September 13, 2021
Accepted September 17, 2021

The results of research on modeling thermodynamic parameters of shock-wave loading of carbides with different stoichiometric ratios are presented. The carbides are considered as a mixture of carbon with the corresponding component. The calculations of pressure, compression and temperature values under shock-wave loading for solid and porous carbides in the range of pressure values above 3 GPa are performed. The model calculations are compared with the known experimental results on the shock-wave loading of carbides with different porosity values. The possibility of modeling the behavior according to the proposed method for carbides for which there are no experimental data at high dynamic loads is shown.

Keywords: Equation of state, shock adiabat, thermodynamic equality, porous heterogeneous medium, carbides

DOI: 10.21883/TP.2022.01.52536.200-21

Introduction

High-temperature composite materials are the most efficient solutions to a great number of problems in high-technology industry. Samples based on oxide-free high-melting compounds (borides, carbides, nitrides) are now being studied extensively. Using the powder (ceramic powder included) processing technology, one may fabricate various composite materials with different practical applications from these high-melting compounds [1]. A number of studies focused on carbides and materials with carbide components have already been published (see, e.g., [2–26]). One of the avenues of research into the compressibility of carbides is related to the problems of explosive compaction of carbide powders and fabrication of microsamples of these compounds with the hardness of the initial grains of samples [2].

Boron carbide B_4C, which is second only to diamond in hardness [3–17], is a carbide material that attracts much interest in the context of fabrication of ceramics and composites. Although the research into shock compression of B_4C has been initiated a long time ago in [3–5], the issue of the presence of a phase transition in the pressure interval from 10 to 100 GPa remains controversial. The possibility of a phase transition in boron carbide subjected to shock compression was first discussed in [6]. Hypotheses regarding the phase transformations of boron carbide under shock compression were formulated in [7,8] based on the presence of kinks in the shock adiabat. Although the authors [7] follow earlier studies in hypothesizing the presence of one or several phase transitions, they note that these experiments do not provide clear evidence of transitions. Experimental data agree with the presence of a phase transition with a slight change in volume at a pressure of approximately 40 GPa. It was suggested in [8] that B_4C differs from other materials in that the jagged structure does not emerge in the shock-wave profile. The change in structure or the mechanism of this phase transition may differ from those in other brittle materials due to the unique crystal structure. Further experiments on static and shock compression are needed to gain a clear understanding of the transition [8]. The concepts of shock-wave loading of boron carbide at pressures up to 90 GPa were reviewed in [9]. It was found that the pressure of phase transformation of shock-compressed boron carbide is hard to determine accurately due to the wide scatter of experimental data stemming from the differences in stoichiometry, porosity, and methods of fabrication of samples. The authors of [9] note that their conclusion regarding the possibility of a phase transition are disputable, but represent a rational estimate of the shock wave and supporting evidence. It is noted that B_4C is (and will likely remain to be) one of the most cryptic ceramics studied with shock-wave techniques [9]. The hypothesized phase transformation with a jump-like change in volume in shock compression of crystalline B_4C was not observed in experiments on static compression [10], where the equation of state and the compression mechanism of almost stoichiometric B_4C have been examined up to the maximum quasi-hydrostatic pressure of 74 GPa. The experiments on bulk compression of B_4C also do not reveal any phase transitions up to 70 GPa [11]. At the same time, it was noted in [12] that the complex of all available experimental data reveals a plateau at a wave velocity of 12.5 km/s. This suggests the presence of a high-pressure phase. A kink in the shock adiabat of B_4C at a pressure of 100 GPa was identified in [13] and associated with the onset of melting of B_4C under shock compression.

In addition to their high hardness, carbides are characterized by a high melting point. High-melting carbides with high hardness and resistance to corrosion are the

basis for the fabrication of high-temperature materials. In nuclear technology, the protective coating of particle fuel for high-temperature reactors is fabricated from carbide and graphite layers intended for long-term operation at high temperatures [18]. The properties of uranium-carbon (UC) systems need to be understood not only in the context of their potential applications in the atomic energy industry, but also from the perspective of fundamental science. However, little experimental and theoretical data on the behavior of UC at high pressures have been published [19–23]. The same is true for other high-melting carbides (specifically, tantalum and hafnium carbides TaC and HfC and their mixtures that feature anomalously high melting points around 4000 K and retain high strength and durability under extreme thermal loads). It was noted in [24] that literature data on the properties of these carbides at high temperatures, which arise in emergency operation modes, are scarce at present. This makes it difficult to simulate such modes and exercise emergency control.

As was noted in [25], „superhard ceramics . . . are often used under conditions of intense shock loads. Due to the high cost of complex ceramic products, forecasting the results of shock impacts by computer simulation becomes a topical problem."One of the possible ways to simulate the behavior of carbides was demonstrated in [26] where carbides were regarded as a mixture of components in the composition of the studied sample. The mixture model, which assumes that components are compressed in a mixture in the same way as pure materials, provided an opportunity to characterize correctly the results of shock-wave experiments for solid carbides with equal stoichiometric ratios of components (WC, TiC, TaC, NbC, SiC, ZrC). Titanium carbide TiC attracts attention as being a high-melting, ultrahard, and wear-resistant material with high electric conductivity and corrosion resistance [27–30]. Alongside with high-strength and high-density alloys based on tungsten, which demonstrate high penetration strength upon shock interaction, porous composite tungsten-based materials alloyed with high-strength components of the type of tungsten carbides present some features of interest [31,32].

In view of the need to determine the parameters of carbides with different porosity values under high dynamic loads and the scarcity (or lack) of experimental data for certain carbides, it seems necessary to develop a sufficiently simple model providing reliable estimates of thermodynamic characteristics of complex materials under load. Specifically, the interaction of components should be taken into account in the description of porous materials, but the mixture method does not allow for this. The thermodynamic equilibrium TEC (thermodynamic equilibrium components) model was examined in [33–37] with reference to a number of materials, including carbides [14].

The aim of the present study is to simulate the shock-wave loading of carbides with different porosities. The studied material is regarded as a mixture of its constituent components. This approach provides an opportunity both to characterize the experimental data for carbides with different stoichiometric ratios of components and to determine the thermodynamic characteristics of shock-wave loading of carbides that had not been studied earlier.

1. Calculation procedure

The TEC model is used to characterize the shock-wave loading of carbides regarded as a mixture of components. This model is based on the assumption that all components of the mixture (including the gas in pores) are in thermodynamic equilibrium, which implies the equality of velocities, pressures, and temperatures. The Mie–Grüneisen equation of state is used in the considered model to characterize the behavior of condensed phases. The equations defining the state of the condensed component are written down:

$$P(\rho, T) = P_C(\rho) + P_T(T), \tag{1}$$

$$P_T(\rho, T) = \Gamma\rho\, E_T(T), \quad E_T(T) = c_V(T - T_0), \tag{2}$$

where P_C is the potential component of pressure, P_T, E_T are the thermal components of pressure and specific energy, c_V is the thermal capacity, and T_0 is the initial temperature. The equation of state for the condensed component with current and initial densities ρ, ρ_0 and the corresponding coefficients A, k then takes the form

$$P(\rho, T) = A\left(\left(\frac{\rho}{\rho_0}\right)^k - 1\right) + \Gamma c_V(T - T_0)\rho. \tag{3}$$

The pressure and the internal energy under normal conditions ($\rho = \rho_0$, $T = T_0$) are assumed to equal to zero in the considered model. Temperature-dependent function $\Gamma = P_T V/E_T$, which defines the contribution of thermal components, is introduced into the equation of state to characterize the behavior of materials of different porosities. This function has the form

$$\Gamma(T) = \left[\left(\Gamma(T_0) - \Gamma(T_\infty)\right)^{-1} + C(T - T_0)\right]^{-1} + \Gamma(T_\infty), \tag{4}$$

$$C = \left([\Gamma(T_*) - \Gamma(T_\infty)]^{-1} - [\Gamma(T_0) - \Gamma(T_\infty)]^{-1}\right)(T_* - T_0)^{-1}. \tag{5}$$

Parameters $\Gamma(T_0)$, $\Gamma(T_*)$, and $\Gamma(T_\infty)$ are chosen according to the condition of correspondence between the shock adiabat and the available experimental data for the studied samples:

$$\Gamma(T) \to \Gamma(T_0) \quad \text{at} \quad T \to T_0,$$

$$\Gamma(T) \to \Gamma(T_\infty) \quad \text{at} \quad T \to T_\infty.$$

$\Gamma(T_0)$ is set on the basis of the available data under normal conditions. The value of $\Gamma(T_*)$ corresponds to temperature $T = T_*$, and asymptotic value of $\Gamma(T_\infty)$ corresponds to the temperature under maximum compression $T = T_\infty$.

The perfect gas equation is taken for gas. At the wave front, the conditions of conservation of mass, momentum,

Parameters of the TEC model

Material	A, GPa	ρ, g/cm^3	k	c_v, J/(kg · K)	$\Gamma(T_0)$	$\Gamma(T_*)$	T_*, K · 10^3	$\Gamma(T_\infty)$
C	200.0	3.515	2.6	500	1.10	0.55	20	0.500
W	101.8	19.235	3.105	140	1.61	1.35	23	0.0
Nb	52.0	8.586	3.2	280	1.68	1.20	23	0.500
B	115.0	2.340	1.7	816	1.10	0.90	23	0.500
Ta	54.18	16.656	3.45	140	1.69	1.15	23	0.667
U	35.0	19.040	4.0	180	1.83	1.20	23	0.500
Mo	95.0	10.206	3.0	294	1.58	1.15	23	0.500

and energy (Hugoniot conditions) are written down [38]. The conditions of conservation of momentum and energy are applied to the mixture as a whole, and the conditions of mass-flux conservation are written down for each component of the mixture. This approach provides an opportunity to simulate the compression both of the material as a whole and of each component separately. The following expression was obtained for a mixture of n condensed components with initial volume fractions μ_{n0}:

$$P = \frac{\sum\limits_{i=1}^{n} A_i \frac{\mu_{i0}}{\sigma_i}\left[\left(h_i - \frac{k_i+1}{k_i-1}\right)\sigma_i^{k_i} + \frac{2k_i\sigma_i}{k_i-1} - h_i - 1\right]}{\sum\limits_{i=1}^{n} \frac{\mu_{i0}}{\sigma_i} h_i + \left(\frac{h_g}{\sigma_g}\right)\left(1 - \sum\limits_{i=1}^{n} \mu_{i0}\right) - 1},$$

$$h_i = \frac{2}{\Gamma_i} + 1, \quad h_g = \frac{2}{\gamma - 1} + 1. \tag{6}$$

Here, $\sigma_i = \rho_i/\rho_{i0}$, $\sigma_g = \sigma_g/\sigma_{g0}$ are the compression ratios of components $i = 1 \ldots n$, ρ_g, ρ_{g0} are the current and the initial densities of gas, and $\gamma = 1.41$ is the adiabatic index. Taken together with the condition of equality of temperatures of components and the equations of state of each component, the obtained equation is sufficient to determine the dependence that may be regarded as the shock adiabat of a multicomponent mixture. In order to simulate the behavior of a solid material, one needs to set the volume fraction of gas to zero. A pure material is regarded as a mixture with a single condensed component. This provides an opportunity to determine the parameters for the components of studied materials. The equations of state of pure materials obtained this way allow one to characterize accurately the results of shock-wave experiments.

2. Simulation results

The availability of experimental data allowed us to verify the considered model and examine the possibility of its application to materials with insufficient (or no) experimental data available for them. The adiabats of components were used in calculations to characterize the shock-wave loading of carbides. Just as in [26], the diamond adiabat was used for carbon. The parameters of the model determined based on the experimental data for components of the studied carbides are presented in the table.

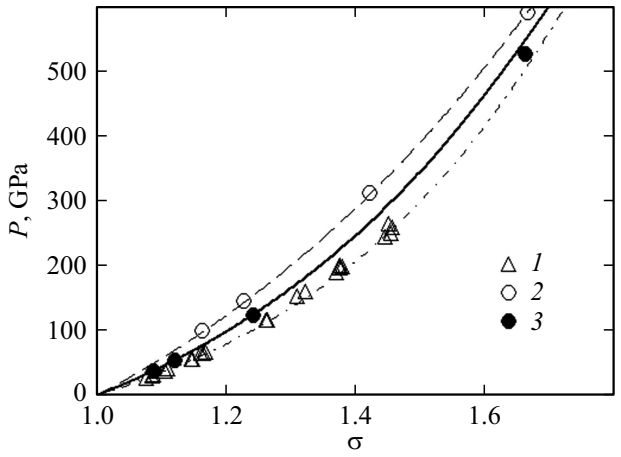

Figure 1. Shock adiabats for diamond (dashed curve), tungsten (dash-and-dot curve), and tungsten carbide WC (solid curve). Experimental data: *1, 3* — [39]; *2* — [40].

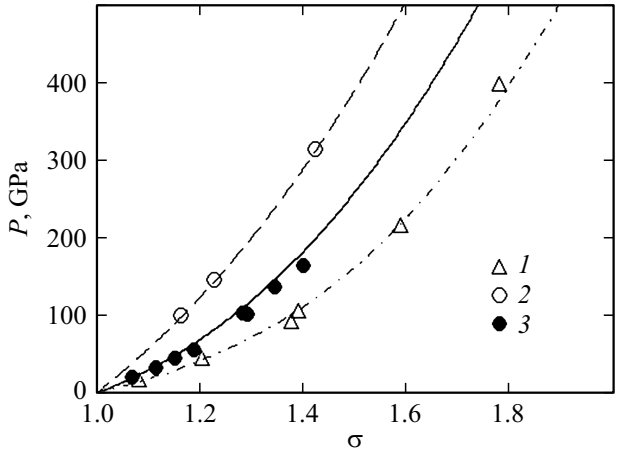

Figure 2. Shock adiabats for diamond (dashed curve), niobium (dash-and-dot curve), and niobium carbide NbC (solid curve). Experimental data: *1* — [39], *2* — [40], *3* — [2].

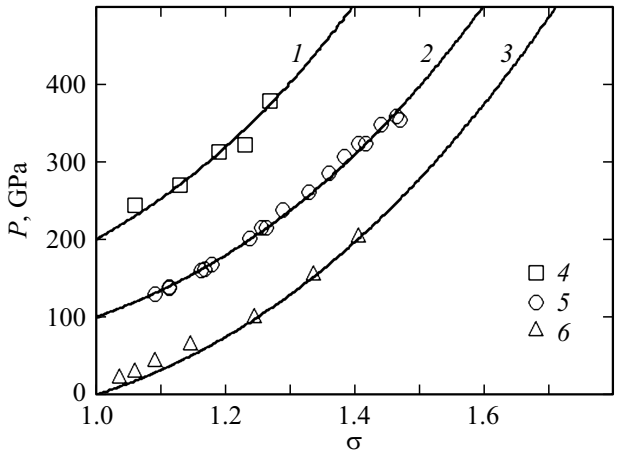

Figure 3. Shock adiabats of porous carbides. Calculated data for WC ($m = 1.201$) — *1*, TaC ($m = 1.125$) — *2*, and NbC ($m = 1.07$) — *3*. Experimental data: *4* — [42], *5* — [41], *6* — [2].

The results of numerical modeling and the experimental data for tungsten carbide WC ($\rho_0 = 15.66\,\mathrm{g/cm^3}$) and niobium carbide NbC ($\rho_0 = 7.8\,\mathrm{g/cm^3}$) are shown in Figs. 1 and 2 in pressure–compression coordinates. Compression σ is defined as the ratio of the initial sample density to the current density. The shock adiabats and the experimental data for components of carbides are presented in the same figures. The volume fractions of components used in the model for carbides were determined based on the stoichiometric ratio of elements. The simulation results agree with the experimental data and the results of calculations performed earlier for solid carbides [26] with equal fractions of such components.

Our approach allowed us to characterize the experimental results both for solid carbides (as in [26]) and for porous samples. A porous carbide is regarded as a porous mixture of components of the corresponding carbide elements. The ratio of volume fractions of condensed components decreases in proportion to porosity m of the sample (porosity m is the ratio of the density of a solid substance to the density of the sample). The results of modeling for carbides with different porosities are presented in Fig. 3. The behavior of tungsten carbide with porosity $m = 1.201$, tantalum carbide ($m = 1.125$), and niobium carbide ($m = 1.07$) was characterized accurately within the accuracy of the experiment. For clarity, the calculated and experimental data are presented with a shift of 100 GPa in pressure.

The assumption of possibility of determination of the volume of components based on the stoichiometric ratio allowed us to characterize accurately the experimental data for boron carbide B_4C (see Fig. 4). The volume fractions for B_4C were determined, in accordance with the chemical composition, in the ratio of 4 : 1.

This approach makes it possible to characterize accurately the experimental data obtained under intense dynamic loads for both solid and porous B_4C samples. The calculated data, the corresponding experimental results [3,7,41], and the data provided by Dudoladov [42] for boron carbide samples with different porosities are presented in Fig. 5 ($m = 1$ for the solid sample). The results of simulation allow us to conclude that the calculated curves agree fairly well with the experimental data in the considered pressure range that is of interest for research into shock-wave synthesis. The deviation of calculated curves from experimental data at porosities $m = 1.16$ and $m = 1.29$ may be attributed to the fact that the accuracy of experimental data decreases at higher porosity values.

The obtained results suggest that the same method may be used to model the thermodynamic parameters of carbides with different stoichiometric ratios with no experimental data available for them. Such calculations of thermodynamic characteristics were performed for uranium carbide UC with equal fractions of these components. The volume fractions were determined in the ratio of 1 : 1.

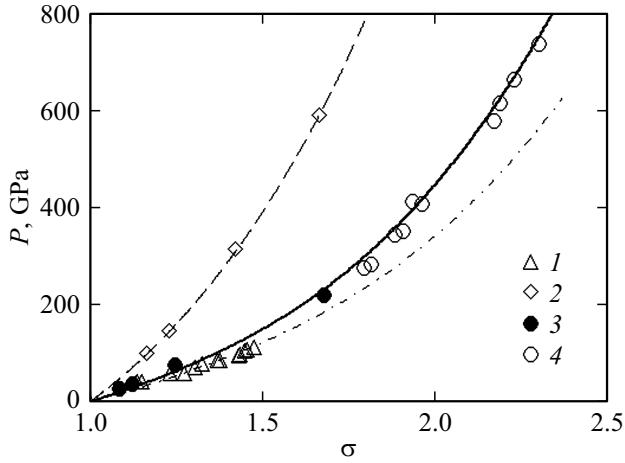

Figure 4. Shock adiabats for diamond (dashed curve), boron (dash-and-dot curve), and boron carbide B_4C (solid curve). Experimental data: *1* — [41]; *2* — [40], *3* — [3], *4* — [12].

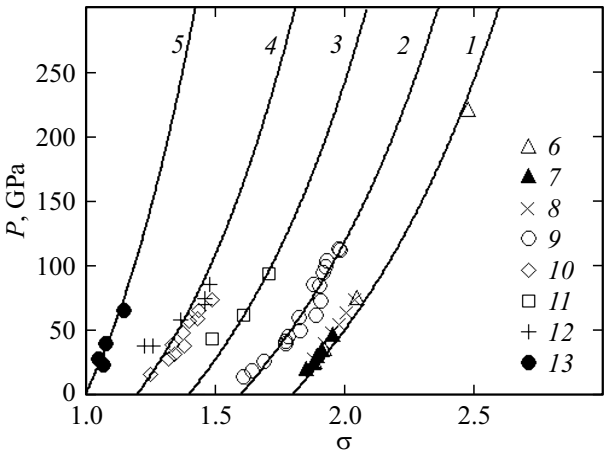

Figure 5. Shock adiabats for porous boron carbide B_4C. Calculated data for porosity $m = 1$ — *1*, $m = 1.046$ — *2*, $m = 1.16$ — *3*, $m = 1.29$ — *4*, $m = 1.74$ — *5*. Experimental data: *6* — [3]; *7, 8* — [7]; *9, 10* — [41]; *11–13* — [42].

The results of modeling for solid carbide UC and the calculated data for components are presented in Fig. 6. The experimental data for components are also shown for illustrative purposes [39–41]. In the case of uranium, the experimental data for materials with density values differing by less than 1% from the density of solid samples were used.

Similar calculations were performed for molybdenum carbide Mo_2C, which has a high melting point. The volume fractions for this carbide were determined in the ratio of 2 : 1. The results of modeling for solid carbide Mo_2C and the calculated and experimental data for components are presented in Fig. 7.

The obtained results suggest the possibility of characterizing the dynamic parameters (pressure, compression) of solid and porous carbides with different stoichiometric ratios under shock-wave loading. In order to model porous carbide samples, one needs to reduce the ratio of volume fractions of condensed components in proportion to the porosity.

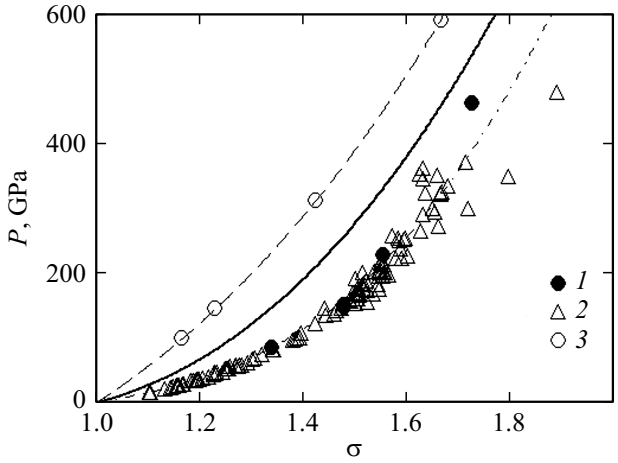

Figure 6. Shock adiabats for diamond (dashed curve), uranium (dash-and-dot curve), and uranium carbide UC (solid curve). Experimental data: *1* — $m = 1.006$ [41]; *2* — $m = 1.005$ [39], *3* — [40].

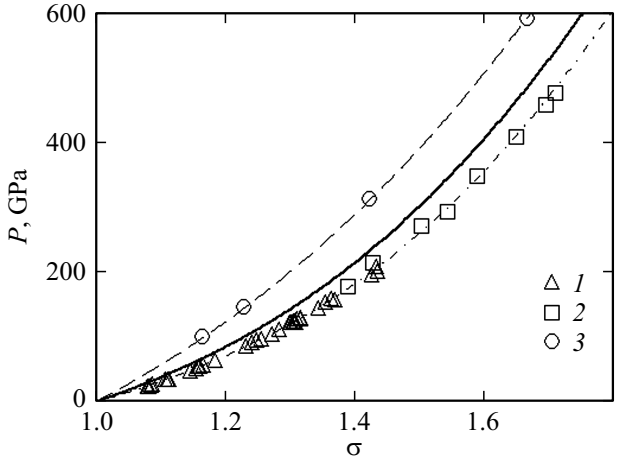

Figure 7. Shock adiabats for diamond (dashed curve), molybdenum (dash-and-dot curve), and molybdenum carbide Mo_2C (solid curve). Experimental data: *1* — [41]; *2* — [39], *3* — [40].

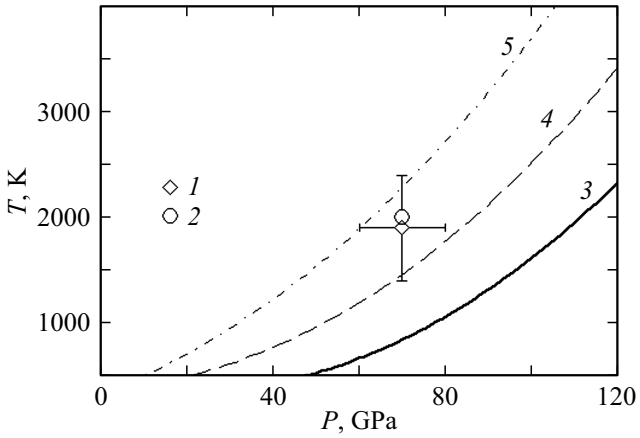

Figure 8. Temperature plotted against pressure along the shock adiabat for boron carbide. Data: *1* — [43], *2* — [44]. Calculations: solid curve *1* for $m = 1$, dashed curve *4* for $m = 1.03$, dash-and-dot curve *5* for $m = 1.07$.

It is instructive to compare the temperature along the shock adiabat of B_4C with different porosity values to one result from [43] (where the temperature at pressure 70 GPa, which is regarded as the region of a phase transition, is given), and the results of molecular dynamics simulations [44] (see Fig. 5 in [43]) for shock-compressed boron carbide. The results of model calculations and the data from [43,44] are presented in Fig. 8. The results of modeling for porosities $m = 1.03$, 1.07 were also added. It can be seen that the calculated values of temperature for solid carbide with $m = 1$ at 70 GPa are lower than those obtained in [43,44]. The latter values are located in the region between the adiabats corresponding to porosities $m = 1.03$, 1.07, which may be interpreted as the region of the shock adiabat of the high-pressure phase. As was demonstrated for carbon [45] (diamond is assumed to be the corresponding high-pressure phase), the experimental values lying above the region of the phase transition are close to the shock adiabat of diamond of the same initial density as the studied carbon samples. This implies that one should consider the shock adiabat for the high-pressure phase with the density lower than that of a solid material. Thus, the shock adiabat of carbide with porosity $m = 1.05$ may be regarded as the one corresponding to the high-pressure phase with an accuracy of 0.02. This confirms indirectly the possibility of a phase transition at this pressure.

A constant thermal capacity for components is used in equation of state (3) of the present model. As was noted in [46], this assumption may be regarded as justified at compression values below 2. Although this results in a certain overestimation of temperature of the studied samples, the dynamic parameters of nitrides (such as pressure and compression within the pressure range of 3–800 GPa) were characterized correctly. It should

be noted that this model allows one to characterize the pressure, compression, and temperature of a loaded medium (including mixtures with their components undergoing a polymorphic phase transition [47,48]). In view of the possibility of a phase transition of carbon, which was mentioned in [26] („the position of the initial section of wave–mass velocity dependences may also be affected by the transition of carbon into the diamond phase, which apparently occurs under these conditions"), it is reasonable to expect that an accurate description of shock-wave loading for carbides undergoing a phase transition under high-energy impact should also be feasible.

Conclusion

Thus, it was demonstrated that the proposed model allows one to characterize the dynamic loading of carbides with different porosities regarded as mixtures of components corresponding to the chemical composition of these carbides. Correct descriptions were obtained both for carbides with equal fractions 1 : 1 in the stoichiometric ratio and for boron carbide with a ratio of 1 : 4. The same method may be used to model the thermodynamic parameters of carbides with different stoichiometric ratios with no experimental data available for them. This approach may be used in numerical modeling of the behavior of complex materials (specifically, carbides) at high energy densities.

Conflict of interest

The author declares that he has no conflict of interest.

References

[1] F.A. Akopov, M.A. Adrianov, R.Kh. Amirov, T.I. Borodina, L.B. Borovkova, G.E. Val'yano, A.Yu. Dolgoborodov, V.V. Tkachenko, M.B. Shavelkina. Refract. Ind. Ceram., **57** (5), 496 (2017). DOI: 10.1007/s11148-017-0011-5

[2] A.A. Bakanova, V.A. Bugaeva, I.P. Dudoladov, R.F. Trunin, Izv. Akad. Nauk SSSR. Ser. Fiz. Zemli, **6**, 58 (1995) (in Russian).

[3] M.N. Pavlovskii, Fiz. Tverd. Tela, **12** (7), 2175 (1970) (in Russian).

[4] R.G. McQueen, S.P. Marsh, J.W. Taylor, J.N. Fritz, W.J. Carter. *The Equation of State of Solids from Shock Wave Studies / In: High Velocity Impact Phenomena,* ed. by R. Kinslow (Academic Press, NY., 1970)

[5] W.H. Gust, E.B. Royce. J. Appl. Phys., **42**, 276 (1971). DOI: 10.1063/1.1686902

[6] D. Grady. J. Phys. IV Proceedings, EDP Sci., **04** (C8), C8-385-C8-391 (1994). DOI: 10.1051/jp4:1994859

[7] T.J. Vogler, W.D. Reinhart, L.C. Chhabildas. J. Appl. Phys., **95**, 4173 (2004). DOI: 10.1063/1.1686902

[8] Y. Zhang, T. Mashimo, Y. Uemura, M. Uchino, M. Kodama, K. Shibata, K. Fukuoka, M. Kikuchi, T. Kobayashi, T. Sekine. J. Appl. Phys., **100**, 113536 (2006). DOI: 10.1063/1.2399334

[9] D.E. Grady. J. Appl. Phys., **117**, 165904 (2015). DOI: 10.1063/1.4918604

[10] P. Dera, M.H. Manghnani, A. Hushur, Yi. Hu, S. Tkachev. J. Solid State Chem., **215**, 85 (2014). DOI: 10.1016/j.jssc.2014.03.018

[11] S.A. Dyachkov, A.N. Parshikov, M.S. Egorova, S.Yu. Grigoryev, V.V. Zhakhovsky, S.A. Medin. J. Appl. Phys., **124**, 085902 (2018). DOI: 10.1063/1.5043418

[12] D.E. Fratanduono, P.M. Celliers, D.G. Braun, P.A. Sterne, S. Hamel, A. Shamp, E. Zurek, K.J. Wu, A.E. Lazicki, M. Millot, G.W. Collins. Phys. Rev. B, **94**, 184107 (2016). DOI: 10.1103/PhysRevB.94.184107

[13] A.M. Molodets, A.A. Golyshev, D.V. Shakhrai. J. Exp. Theor. Phys., **80**, 467 (1995). DOI: 10.1134/S1063776117030049

[14] K.K. Maevskii. AIP Conf. Proc., **2167**, 020204 (2019). DOI: 10.1063/1.5132071

[15] A.S. Savinykh, I.A. Cherepanov, S.V. Razorenov, A.I. Ovsienko, V.I. Rumyantsev, S.S. Ordan'yan. Tech. Phys., **63**, 1755 (2018). DOI: 10.1134/S1063784218120186

[16] R.Kh. Bagramova, N.R. Serebryanaya, V.M. Prokhorov, V.D. Blank. Tech. Phys., **63** (7), 1010 (2018). DOI: 10.1134/S1063784218070046

[17] A.S. Savinykh, G.V. Garkushin, S.V. Razorenov, V.I. Rumyantsev. Tech. Phys., **60**, 863 (2015). DOI: 10.1134/S1063784215060249

[18] A.I. Savvatimskii, S.V. Onufriev. High Temp., **58**, 800 (2020). DOI: /10.1134/S0018151X20060188

[19] B.D. Sahoo, K.D. Joshi, T.C. Kaushik. Comput. Condens. Matter., **21**, e00431 (2019). DOI: 10.1016/j.cocom.2019.e00431

[20] J.S. Olsen, L. Gerward, U. Benedict, J.-P. Itié, K. Richter. J. Less Common Metal., **121**, 445 (1986). DOI: 10.1016/0022-5088(86)90561-8

[21] B.D. Sahoo, K.D. Joshi, Satish C. Gupta, J. Nucl. Mater., **437**, 81 (2013). DOI: 10.1016/j.jnucmat.2013.01.314

[22] B.D. Sahoo, D. Mukherjee, K.D. Joshi, T.C. Kaushik. J. Appl. Phys., **120**, 085902 (2016). DOI: 10.1063/1.4961497

[23] J.-P. Dancausse, S. Heathman, U. Benedict, L. Gerward, J. Staun Olsen, F. Hulliger J. Alloy. Compd., **191**, 309 (1993). DOI: 10.1016/0925-8388(93)90084-Z

[24] V.N. Senchenko, R.S. Belikov. J. Phys.: Conf. Ser., **1147**, 012011. (2019). DOI: 10.1088/1742-6596/1147/1/012011

[25] A.S. Savinykh, I.A. Cherepanov, S.V. Razorenov, K. Mandel, L. Krüger. Tech. Phys., **64**, 356 (2019). DOI: 10.1134/S1063784219030216

[26] R.F. Trunin, *Issledovaniya ekstremal'nykh sostoyanii kondensirovannykh veshchestv metodom udarnykh voln. Uravneniya Gyugonio* (RFYaTs–VNIIEF, Sarov, 2006), p. 137 (in Russian).

[27] A.Ya. Pak, T.Yu. Yakich, G.Ya. Mamontov, M.A. Rudmin, Yu.Z. Vasil'eva. Tech. Phys., **65**, 771 (2020). DOI: 10.1134/S1063784220050205

[28] S.A. Rasakia, B. Zhanga, K. Anbalgamb, T. Thomas, M. Yang. Prog. Solid State Chem., **50**, 1 (2018) DOI: 10.1016/j.progsolidstchem.2018.05.001

[29] D. Cho, J.H. Park, Y. Jeong, Y.L. Loo. Ceram. Int., **41**, 10974 (2015) DOI: 10.1016/j.ceramint.2015.05.041

[30] Q. Dong, M. Huang, C. Guo, G. Yu, M. Wu. Int. J. Hydrogen Energy, **42**, 3206 (2017) DOI: 10.1016/j.ijhydene.2016.09.217

[31] A.N. Ishchenko, S.A. Afanas'eva, N.N. Belov, V.V. Burkin, S.V. Galsanov, V.Z. Kasimov, V.A. Kudryavtsev, Ya.D. Lipatnikova, L.S. Martsunova, K.S. Rogaev, A.Yu. Sammel', A.B. Skosyrskii, N.T. Yugov. Tech. Phys., **65**, 414 (2020). DOI: 10.1134/S106378422003010X

[32] A.S. Savinykh, K. Mandel, S.V. Razorenov, L. Krüger. Tech. Phys., **63**, 357 (2018). DOI: 10.1134/S1063784218030210
[33] K.K. Maevskii. J. Phys. Conf. Series., **894**, 012057 (2017). DOI: 10.1088/1742-6596/894/1/012057
[34] K.K. Maevskii, S.A. Kinelovskii. High Temperature, **56** (6) 853 (2018). DOI: 10.1134/S0018151X18060172
[35] K.K. Maevskii, S A Kinelovskii. J. Phys. Conf. Series., **946**, 012113 (2018). DOI: 10.1088/1742-6596/946/1/012113
[36] K.K. Maevskii. Math. Montis., **41**, 123 (2018).
[37] K.K. Maevskii. Tech. Phys., **66**, 791 (2021). DOI: 10.1134/S1063784221050145
[38] Ya.B. Zel'dovich, Yu.P. Raizer, *Fizika udarnykh voln i vysokotemperaturnykh gidrodinamicheskikh yavlenii* (Fizmatlit, M., 2008), p. 519 (in Russian).
[39] P.R. Levashov, K.V. Khishchenko, I.V. Lomonosov, V.E. Fortov. AIP Conf. Proc., **706**, 87 (2004). http://www.ihed.ras.ru/rusbank/
[40] M.N. Pavlovskii, Fiz. Tverd. Tela, **13** (3), 893 (1970) (in Russian).
[41] S.P. Marsh (editor). *LASL Shock Hugoniot Data* (Univ. California Press, Berkeley, 1980)
[42] R.F. Trunin, L.F. Gudarenko, M.V. Zhernokletov, G.V. Simakov, *Eksperimental'nye dannye po udarno-volnovomu szhatiyu i adiabaticheskomu rasshireniyu kondensirovannykh veshchestv* (RFYaTs–VNIIEF, Sarov, 2006) (in Russian).
[43] A.M. Molodets, A.A. Golyshev, G.V. Shilov. JETP Lett., **111** (12), 720 (2020). DOI: 10.1134/S0021364020120103
[44] M. DeVries, G. Subhash, A. Awasthi. Phys. Rev. B, **101**, 144107 (2020). DOI: 10.110
[45] I.V. Lomonosov, V.E. Fortov, A.A. Frolova, K.V. Khishchenko, A. A. Charakhchyan, L.V. Shurshalov. Tech. Phys., **48**, 727 (2003). DOI: 10.1134/1.1583826
[46] A.V. Ostrik, Konstr. Kompoz. Mater., **2**, 48 (2018) (in Russian).
[47] K.K. Maevskii, S.A. Kinelovskii. AIP Conf. Proc., **1783**, 020143 (2016). DOI: 10.1063/1.4966436
[48] K.K. Maevskii. Math. Montis., **50**, 140 (2021). DOI: 10.20948/mathmontis-2021-50-12